Materials Science Forum Vol. 502 (December 2005) pp. 499-504
online at http://www.scientific.net

Analysis of Laser Fusion Zone of Lotus-type Porous Metals by 3-dimensional FEM

Takuya Tsumura[1,a], Taichi Murakami[2,b], Soong-Keun Hyun[3,c], Hideo Nakajima[3,d] and Kazuhiro Nakata[1,e]

[1]Joining and Welding Research Institute, Osaka University, 11-1 Mihogaoka, Ibaraki, Osaka 567-0047, Japan

[2]Dept. of Materials Processing, Graduate School of Eng., Tohoku University, 02 Aza Aoba, Aramaki, Aoba-ku, Sendai, Miyagi 980-8579, Japan

[3]The Institute of Scientific and Industrial Research, Osaka University, 8-1 Mihogaoka, Ibaraki, Osaka 567-0047, Japan

[a] tsumura@jwri.osaka-u.ac.jp, [b] taichi@material.tohoku.ac.jp, [c]hyun23@sanken.osaka-u.ac.jp, [d]nakajima@sanken.osaka-u.ac.jp, [e]nakata@jwri.osaka-u.ac.jp

Keywords: Lotus-type Porous Metal, Laser Welding, Anisotropy, Thermal Analysis, FEM

Abstract: Effects of pore directions on the profile of fusion zone for lotus-type porous magnesium by laser welding has been investigated by comparing the experimental observations and the results of numerical simulation. The three-dimensional finite element calculations were performed, which takes into account equivalent thermal properties and anisotropy of thermal conductivity. There is the pore anisotropy in the profile of fusion zone by laser beam irradiation and the good weldability was obtained when the growth direction of the original pore equaled to the direction of the laser beam irradiation. A good agreement was obtained between the calculated profile of the weld fusion zone and the experimental results.

1. Introduction

Lotus-type porous metals, whose pores are foamed by supersaturated gas utilizing the difference of gas solubility between liquid and solid and are aligned in one direction by unidirectional solidification, have a unique combination of properties [1-9]. These are expected as the innovative engineering materials, which yield various anisotropic properties depending on alignment of the growth of pores. For the industrial use of the lotus-type porous metals as various parts, a reliable joining technique such as welding is required as well as processing techniques. The authors reported the melting property of the lotus-type porous copper [10] and magnesium [11] by laser beam irradiation. These indicated that these materials possessed anisotropy of melting property with the pore perpendicular and parallel to the work piece surface owing to the difference of the laser energy absorption to the specimen and the anisotropy of the thermal conductivity. The aim of this study is to elucidate the effect of the pore growth direction on the melting property by comparing the result of numerical simulation and the experimental observations.

2. Finite Element Modeling of Lotus-type Porous Metals

Thermal analysis of a three-dimensional finite element model under the non-steady-state conditions was carried out so as to evaluate the melting property of the lotus-type porous metals. The analyses are performed using a commercial FEM code, ABAQUS.

It is assumed that the lotus-type porous metal is an equivalent homogeneous orthotropic material, in which the principal axis for material properties is along the aligned direction of pores. With this

assumption, an equation of the heat conductive analysis for this type of material can be expressed by,

$$\rho_{eq}(T)C_{p\,eq}(T)\frac{\partial T}{\partial t}=\frac{\partial}{\partial x}\left(\lambda_{x\,eq}(T)\frac{\partial T}{\partial x}\right)+\frac{\partial}{\partial y}\left(\lambda_{y\,eq}(T)\frac{\partial T}{\partial y}\right)+\frac{\partial}{\partial z}\left(\lambda_{z\,eq}(T)\frac{\partial T}{\partial z}\right)+\dot{Q}, \tag{1}$$

where $\rho_{eq}(T)$ and $C_{p\,eq}(T)$ are the equivalent density and the equivalent specific heat, respectively, x, y, z are the Cartesian coordinates, $\dot{Q}$ is the internal heat generated per unit volume and time, $\lambda_{i\,eq}(T)_{(i=x,y,z)}$ are the equivalent thermal conductivity at each axis. The symbol (T) indicates a function of temperature, T.

The thermal analysis was conducted using temperature dependence of material properties. However, there is no data of these equivalent properties of the lotus-type porous metal. Therefore, the values of these properties were calculated from that of nonporous metal. On the assumption that the porosity dependence on the thermal property of the lotus-type porous metal is the same as that of copper, the equivalent thermal conductivity of the lotus-type porous metal can be calculated using the relation between the pore growth direction and the porosity dependence of the lotus-type porous copper [9]. Furthermore, assuming the temperature dependence of the equivalent thermal conductivity is independent of the pore growth direction and porosity, equations of the equivalent thermal conductivity of the lotus-type porous metal are expressed by,

$$\lambda_{eq}^{//}(T)=(1-\varepsilon)\lambda_n(T),\quad \lambda_{eq}^{\perp}(T)=\frac{(1-\varepsilon)}{(1+\varepsilon)}\lambda_n(T), \tag{2}$$

where $\lambda_{eq}^{//}(T)$ and $\lambda_{eq}^{\perp}(T)$ are the equivalent thermal conductivity parallel and perpendicular to pores, respectively, ε is the porosity of the lotus-type porous metal, and $\lambda_n(T)$ is the thermal conductivity of nonporous metal. On the same assumptions, the equivalent density and the equivalent specific heat of the lotus-type porous metal were calculated by following equations,

$$\rho_{eq}(T)=(1-\varepsilon)\rho_n(T),\quad C_{p\,eq}(T)=(1-\varepsilon)C_{p\,n}(T), \tag{3}$$

where $\rho_n(T)$ and $C_{p\,n}(T)$ are density and specific heat of nonporous metal, respectively.

The heat input to the weld is generally calculated from the energy supplied at the keyhole. The model of the heat source assumes a uniform density distribution on the weld pool simulated by a half-spheroid. The shape of the keyhole, which changes with time, is defined as the diameter of 0.6 mm and the depth of d mm, which is equaled to that of the weld pool at the laser spot. The initial condition is $t=0$ s, $d=0.3$ mm. Figure 1 shows the flow chart of the determination of the shape of keyhole and the calculation of the temperature distribution. The initial condition is $t=0$ s, T_0=298 K. The heat conduction

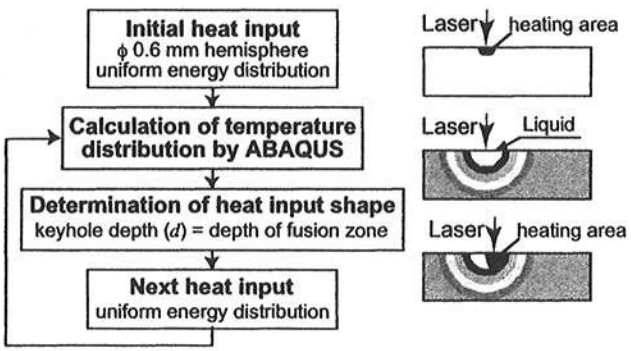

Fig. 1 Flow chart of determination of temperature distribution and keyhole shape.

on the work piece surface is considered as the boundary condition. The heat flux on the work piece surface is defined as follows,

$$q_s = \alpha_c (T - T_0), \tag{4}$$

where T and α_c are temperature on the work piece surface and the heat transfer coefficient of ambient gas, respectively. In this study, α_c is adopted as 1.163W/m^{2}K, which is the minimum value of air without flow. The convection in the weld metal, the radiation of the work piece and the heat transfer by the phase transformation are neglected for the simplification of the calculation.

3. Experimental Procedure

The ingot of lotus-type porous magnesium was 100 mm in diameter and 100 mm in height. The average pore diameter and the porosity of specimens were about 0.15 mm and 35 %, respectively. Thermal conductivity is one of the main factors controlling the profile of weld fusion zone. Therefore, it is expected that the profile of weld fusion zone be affected by the anisotropy of thermal conductivity caused by different pore growth directions. So the work pieces measuring 40 mm × 40 mm with 1.8 mm in thickness were cut out of the ingot with the pore growth perpendicular and parallel to the work piece surface using a spark-erosion wire-cutting machine (Brother Industries Ltd., HS-300).

Figure 2 shows schematic views of specimens during laser welding. The laser beam was delivered using an optical fiber with a diameter of 0.3 mm. The welding of the work piece was conducted using an Nd: yttrium-aluminum-garnet (Nd: YAG) laser unit with a maximum output power of 3.2 kW in continuous wave mode. The laser beam power was 1.0 kW with the spot diameter of 0.6 mm. The welding speed was controlled in 83.3 mm/s. Argon was used as a shielding gas with a flow rate of 5.0×10^{-4} m^3/s. The cross-section of the welded specimen was observed by light microscope to determine the profile of the weld fusion zone.

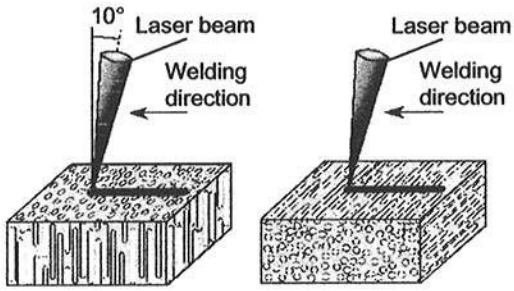

(a) perpendicular direction (b) parallel direction

Fig. 2 Schematic views of specimens during laser welding in the porous metal.

4. Results and Discussions

4.1 Results of Numerical Simulation. The laser power irradiated to the work piece surface is approximately 80 % of the laser beam power, because the optical system of the laser unit absorbs the energy of the laser. Moreover, during laser welding, a part of the laser energy irradiated is lost by the reflection at the work piece surface. The estimation of the energy loss is essential for the calculation of the temperature distribution by the laser welding. However, it is impossible to estimate the energy loss because of no data of the reflection of lotus-type porous magnesium. Because the aim of this calculation is to elucidate the difference of the melting property against the pore growth direction, the energy loss is assumed to be 40 % of the laser power irradiated to the work piece surface. This assumption gives the most agreed results between the calculation and the experiment. Therefore, the effective power supplied to the work piece surface is assumed to be 48 % of the power of the laser source. It was supposed that the size of the specimen, the effective laser power, the welding speed and the spot diameter are 20 mm (x) × 10 mm (y) × 1.8 mm (z), 0.48 kW, 83.3 mm/s and 0.6 mm,

respectively. The analysis region is y>0 due to space symmetry. The size of unit element is 0.25 mm (x) × 0.25 mm (y) × 0.3 mm (z). The average pore diameter of the lotus-type porous magnesium in this study is 0.15 mm, which is the same order as the size of unit element. From the viewpoint of the calculation using the composite, many pores in unit element are required. In this study, however, the preparation of unit element with many pores is impossible because the thickness of the work piece is thin. Therefore, the lotus-type porous magnesium is taken for the nonporous material with anisotropy of thermal conductivity. The thermal conductivity, the density, and the specific heat of nonporous magnesium were cited from [12] [13].

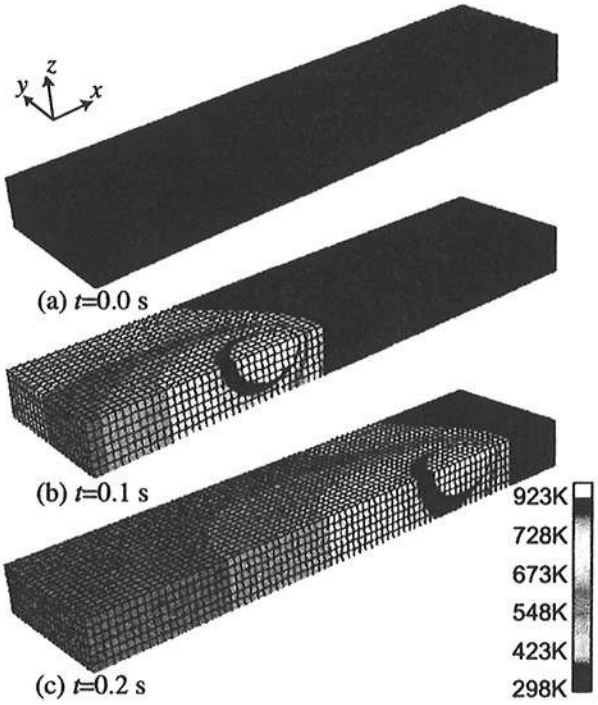

Fig. 3 Calculated temperature distribution of lotus-type porous magnesium with the pores parallel to the work piece surface during laser welding process at three different times. The laser power, the welding speed and the spot diameter are 0.48kW, 83.3mm/s and 0.6mm, respectively.

Figure 3 shows the time change of temperature distribution. Figure 3(a), (b) and (c) are t=0.0 s, 0.1 s and 0.2 s, respectively. The porosity of the work piece is 35 %, and the direction of the pore growth is parallel to the work piece surface. The laser beam power, the spot diameter and the welding speed are 0.48 kW, 0.6 mm and 83.3 mm/s, respectively. The welding time is 0.24 s. The white regions indicate the weld pool with the keyhole. Shortly, it is the profile of weld metal. The profile of white region is mostly constant after t=0.1 s. Therefore, the estimation of the profile of weld metal using cross section of the maximum temperature distribution at x=10 mm was carried out.

4.2 Comparison of Experimental Observations and Numerical Results. Figure 4 shows the cross section of the laser welding seam of lotus-type porous magnesium with the pores perpendicular and parallel to the work piece surface together with calculated maximum temperature field at $x = 10$ mm. From the experimental results, in the perpendicular case, the work piece melted through the bottom. On the other hand, in the parallel case, the depth of the weld metal is approximately 70 % of the work piece thickness. These results reproduce the difference of the profile of weld fusion zone on the pore growth direction. Compared experiment with calculation results, however, the experimental width of the weld metal was smaller than the calculated ones. One reason is the boundary condition. In the experiment, ambient gas is argon with flow because argon was used as a shielding gas. In this analysis, however, ambient gas is air without flow. Therefore, the heat evolution from the work piece surface using calculation is estimated less than actual evolution. This factor scarcely influences the difference of the profile of weld fusion zone on the pore growth direction.

Accordingly, the profile difference between the weld fusion zone of the lotus-type porous magnesium with the pores perpendicular to the work piece surface and parallel one is mainly controlled by anisotropy of thermal conductivity.

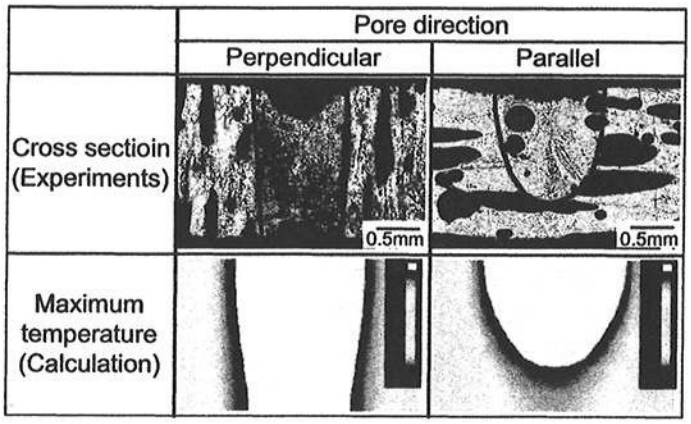

Fig. 4 Comparison between cross section of the laser welding seam of lotus-type porous magnesium and calculated maximum temperature field at the layer 10 mm in length.

5. Conclusions

The melting property of lotus-type porous magnesium with 1.8mm in thick has been studied using Nd:YAG laser welding in the 83.3 mm/s welding speed and 1.0 kW laser power at argon shielding gas and numerical simulation. The obtained results are summarized as follows,

There is the pore anisotropy in the melting property by laser beam irradiation when the work pieces in the perpendicular and parallel pore directions to the work piece surface, on which laser beam was irradiated, were melted.

The three-dimensional finite element calculations were performed, which takes into account temperature dependency and the pore anisotropy of thermal conductivity. A good agreement was obtained between the calculated profile of weld fusion zone and experimental results. It indicates that the difference of the melting property on the pore growth direction against the work piece surface is controlled by the pore anisotropy of thermal conductivity.

References

[1] H. Nakajima: Materials Integration Vol.12 (1999), p. 37

[2] H. Nakajima: The Production & Technique Vol.51 (1999), p. 60

[3] H. Nakajima: Boundary Vol.15 (1999), p. 9

[4] H. Nakajima: J. High Temperature Materials Vol.26 (2000), p. 95

[5] H. Nakajima, S.K. Hyun, K. Ohashi, K. Ota and K. Murakami: Colloids and Surfaces A Vol.179 (2001), p. 209

[6] S.K. Hyun, K. Murakami and H. Nakajima, Mater. Sci. and Eng. A Vol.299 (2001), p. 241

[7] S.K. Hyun, H. Nakajima: Mater. Sci. and Eng. A Vol.340 (2003), p. 258

[8] K. Ota, K. Ohashi and H. Nakajima: Mater. Sci. and Eng. A Vol.341 (2003), p. 139

[9] T. Ogushi, H. Chiba, T. Ikeda and H. Nakajima: Cellular Metals: Manufacture, Properties, Applications, MIT-Verlag (2003), p. 493

[10] T. Murakami, K. Nakata, T. Ikeda, H. Nakajima and M. Ushio: Mater. Sci. and Eng. A Vol.357 (2003) , p.134

[11]T. Murakami, K. Nakata, T. Ikeda, H. Nakajima and M. Ushio: Collected Abstracts of the 2003 Spring Meeting of The Japan Institute of Metals Vol.132 (2003), p. 406 (in Japanese)

[12]Y. S. Touloukian: *Thermophysical properties of matter: Vol.1 Thermal conductivity of metallic elements and alloys* (IFI/Plenum, New York, 1970).

[13]C.J. Smithell et al.: *Metals Reference Book, 6th ed.* (Buteerworth, London, 1983).